Nonresonant enhancement of the nonstationary holographic currents in photoconductive crystals

Mikhail Bryushinin, Vladimir Kulikov, and Igor Sokolov*
A. F. Ioffe Physical Technical Institute, 194021, St. Petersburg, Russia
(Received 12 November 2001; revised manuscript received 16 January 2002; published 31 May 2002)

We report the nonresonant excitation of the nonstationary holographic currents in an external sinusoidal electric field. The theoretical analysis of the effect has been performed for the conventional model of semiconductor with one type of partially compensated donor level. We demonstrate that the application of an ac field sufficiently increases the photocurrent amplitude. At the same time the frequency transfer function of the effect maintains the form typical for the diffusion mechanism of photocurrent excitation. The dependencies of the current amplitude and characteristic cutoff frequency versus applied voltage are utilized for the determination of the photocarrier's $\mu\tau$ product. The advantages of the proposed technique are discussed. The experiments are carried out in a photorefractive *n*-type $Bi_{12}SiO_{20}$ crystal. The signal enhancement of ~ 50 dB has been achieved and the $\mu\tau$ product is found to be $\mu\tau=(0.8-1.2)\times 10^{-10}$ m^2/V.

DOI: 10.1103/PhysRevB.65.245204 PACS number(s): 72.20.Jv, 42.70.Nq

I. INTRODUCTION

Investigation of the space-charge grating formation in semiconductors and, in particular, wide-gap materials is very important since it provides information about the main fundamental characteristics of the material such as type of photoconductivity, Maxwell relaxation time, characteristic transport lengths of photocarriers, volume charge distribution, mobility, and lifetime. There are two modern optical techniques for such measurements. The first one is based on the recording of the dynamic holographic gratings in photorefractive crystals.[1] The amplitude of the space-charge grating can be enhanced using nonstationary mechanisms of recording: the first approach uses application of a dc electric field to the crystal illuminated with a running interference pattern,[2,3] and the second one employs application of an ac electric field along with a stationary interference pattern.[4–6] In both cases the space-charge field grating amplitude grows as $\propto E_0^2$ until saturation or nonlinearity effects become substantial.[1] Both approaches can be utilized for electro-optic materials only since they require light diffraction on the recorded holographic grating.

The nonstationary holographic currents[7] [or non-steady-state photoelectromotive force[8] (photo-EMF)] can be considered as the alternative optical technique. This method does not involve light diffraction from the recorded hologram and can be used for centrosymmetric and even amorphous materials.[9,10] The photo-EMF is the holographic-related phenomenon and reveals itself as an alternating electric current in a semiconductor crystal illuminated by an oscillating interference pattern.[8,11,12] Resonant excitation of the nonstationary holographic currents in an external dc field has already been realized in wide-gap photorefractive sillenites.[13–15] No investigations of the photocurrent excitation in an external ac field has been carried out up to now. The study of the nonstationary holographic currents in an external alternating electric field is useful not only for better understanding of the space-charge field formation and characterization of the wide-gap semiconductors, but also for practical applications, namely, the detection of weakly phase-modulated laser beams, and remote laser testing including laser ultrasonic diagnostics.[16,17] There is also a number of fields where adaptive detection of low-frequency (1–100-Hz) phase-modulated optical signals is necessary. An important example is detection of slow periodic thermal changes in experiments on detection of weak optical absorption.[18] One can use photodetectors with low photoconductivity and large Maxwell relaxation time. But this will result in a low photoresponse of detection and additional problems in matching photodetector with preamplifier. To solve these problems authors of Ref. 14 have suggested the application of dc field for the resonant enhancement of the photocurrent amplitude. In our point of view utilization of the nonresonant technique for the signal amplification presented below is more convenient for the mentioned tasks.

In this paper we present investigations of the nonstationary photocurrent generation in an external ac field. We show both experimentally and theoretically that the frequency transfer function of the effect is similar to the response of the effect in the diffusion regime of excitation, i.e., linear growth of the signal for low modulation frequencies up to a certain characteristic cutoff frequency and frequency-independent region for high modulation frequencies. We propose a technique for the signal enhancement and determination of the $\mu\tau$ product. In Sec. II we analyze theoretically the holographic photocurrents in an external ac electric field, in Sec. III we describe the experimental setup, in Sec. IV we present the results of the nonstationary photocurrent measurements in *n*-type photorefractive $Bi_{12}SiO_{20}$, and in Sec. V we discuss the possibilities of the proposed technique.

II. THEORETICAL ANALYSIS

This section presents calculations of the nonstationary photocurrent amplitude excited in an alternating electric field. Suppose a crystal is illuminated with the oscillating interference pattern formed by two plane light waves, one of which being phase modulated with frequency ω and amplitude Δ:

$$I(x,t)=I_0[1+m\cos(Kx+\Delta\cos\omega t)]. \quad (1)$$

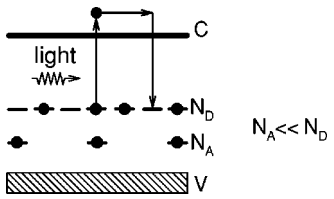

FIG. 1. Model of semiconductor with one type of partially compensated donor level.

Here I_0 is the average light intensity, m is the contrast, and K is the spatial frequency of the interference pattern. We consider the widely used model of semiconductor with one type of partially compensated donor level[1] (Fig. 1). The balance equation for the concentration of electrons in the conduction band n can be written as follows:

$$\frac{\partial n}{\partial t}=g-\frac{n}{\tau}+\frac{1}{e}\frac{\partial j_e}{\partial x}. \tag{2}$$

Here $g(x,t)=(\alpha\beta/h\nu)I(x,t)$ is the electron generation rate (α is the light absorption coefficient, β is the quantum efficiency, and $h\nu$ is the photon energy), τ is the electron lifetime, j_e is the density of the electron current, and e is the electron charge. We assume low illumination levels when the generation and recombination rates are linear functions of the light intensity and electron concentration, respectively, i.e., for the considered model conditions $N_A+N\ll N_D$, $N_A+N\gg n$ that are fulfilled [N_D is the total concentration of donors, N is the concentration of donor centers emptied by light, and N_A is the concentration of the compensating acceptor states (Fig. 1)]. In this case the electron lifetime is independent on the light intensity and determined by the concentration N_A only. The effects of trap saturation are neglected as well (screening lengths are small compared to the inverse value of the spatial frequency). In order to calculate the distributions of the electron concentration, electric field and resulting photocurrent, Eq. (2) should be added by the continuity and Poisson equations and by the expressions for the charge ρ and electron current j_e densities:

$$\frac{\partial \rho}{\partial t}+\frac{\partial j_e}{\partial x}=0, \tag{3}$$

$$\epsilon\epsilon_0\frac{\partial E}{\partial x}=\rho, \tag{4}$$

$$\rho=e(N-n), \tag{5}$$

$$j_e=e\mu nE+k_BT\mu\frac{\partial n}{\partial x}, \tag{6}$$

where E is the electric field, μ is the electron mobility, ϵ is the dielectric constant, and ϵ_0 is the free space permittivity, k_B is the Boltzmann constant, and T is the temperature. Equations (2)–(6) can be represented as follows:

$$\frac{\partial n}{\partial t}=g-\frac{n}{\tau}-\frac{\epsilon\epsilon_0}{e}\frac{\partial^2 E}{\partial x\partial t}, \tag{7}$$

$$\frac{\partial}{\partial x}\left(e\mu nE+k_BT\mu\frac{\partial n}{\partial x}+\epsilon\epsilon_0\frac{\partial E}{\partial t}\right)=0. \tag{8}$$

The sinusoidal electric field with amplitude E_{ext} and frequency Ω is applied to the crystal: $E_{ext}(t)=E_{ext}\cos\Omega t$.

The calculation procedure simplifies substantially if we assume the contrast m and amplitude of phase modulation Δ to be small: $m,\Delta\ll 1$. Then we can look for the solution of Eqs. (7) and (8) to the lowest order with respect to the small parameters presenting $n(x,t)$, $E(x,t)$ as the sums of stationary and running gratings:

$$n=n_0+\sum_{p,q=-1}^{1} n^{+pq}\exp\{i[Kx+(p\omega+q\Omega)t]\}+\sum_{p,q=-1}^{1} n^{-pq}\exp\{i[-Kx+(p\omega+q\Omega)t]\}, \tag{9}$$

$$E=E^{00+}\exp(i\Omega t)+E^{00-}\exp(-i\Omega t)+\sum_{p,q=-1}^{1} E^{+pq}\exp\{i[Kx+(p\omega+q\Omega)t]\}+\sum_{p,q=-1}^{1} E^{-pq}\exp\{i[-Kx+(p\omega+q\Omega)t]\}. \tag{10}$$

It is important to point out that for the solution of similar tasks two basic approaches can be used: the utilization of truncated Fourier series[5] (as was also done in this paper) and the time averaging technique.[4] The former covers all time scales,[19] the latter is convenient for arbitrary wave forms of the external field.[6]

For the case of cyclic boundary conditions[8] the total current averaged over the interelectrode spacing L contains the drift and displacement components. The photocurrent signal is defined by the drift one:[8]

$$j(t)=\frac{1}{L}\int_0^L e\mu n(x,t)E(x,t)dx. \tag{11}$$

We confine ourselves to the analysis of the first harmonic of photocurrent (with frequency ω) which can be written in the form of the following combination of coefficients introduced in Eqs. (9) and (10):

$$j^{\omega}=2e\mu\sum_{q=-1}^{1}(n^{+1q}E^{-0(-q)}+n^{+0q}E^{-1(-q)}+n^{-1q}E^{+0(-q)}+n^{-0q}E^{+1(-q)}). \tag{12}$$

The higher spatial and temporal harmonics (and even subharmonics) of values $n(x,t)$, $E(x,t)$ and resulting photocurrent $j(t)$ become substantial only for the case of large contrast and amplitude of phase modulation: $m,\Delta\sim 1$.[1,20–22] Although these problems are rather interesting and widely discussed in the literature the most valuable applications of the holographic photocurrents for the semiconductor material characterization (Sec. I) are based on the measurements of the first harmonic of the signal.

Let us consider the case of a ''relaxation-type'' semiconductor, i.e., $\tau \ll \tau_M$ ($\tau_M = \epsilon\epsilon_0/e\mu n_0$ is the Maxwell relaxation time). We suppose that the frequency of phase modulation ω is much smaller than the frequency of the external electric field Ω; the period of the ac field is larger than the carrier lifetime τ and shorter than grating relaxation time τ_M:

$$\omega \ll \Omega, \tag{13}$$

$$\tau_M^{-1} \ll \Omega \ll \tau^{-1}. \tag{14}$$

We have obtained all complex amplitudes of the electron concentration and electric field necessary for calculation of the first harmonic of the photocurrent signal. Some of them are given below

$$n^{+00} = \frac{m}{2} n_0, \quad n^{+01} = \frac{imKL_0}{2\sqrt{2}(1+K^2L_D^2)} n_0,$$

$$n^{+10} = \frac{im\Delta(1+i\omega\tau_M)(1+K^2L_D^2)n_0/4}{1+K^2L_D^2+i\omega\tau_M[(1+K^2L_D^2)^2+K^2L_0^2]},$$

$$n^{+11} = \frac{-m\Delta(1+i\omega\tau_M)KL_0 n_0/4\sqrt{2}}{1+K^2L_D^2+i\omega\tau_M[(1+K^2L_D^2)^2+K^2L_0^2]},$$

$$E^{+00} = -i\frac{m}{2}\left(E_D + E_0\frac{KL_0}{1+K^2L_D^2}\right),$$

$$E^{+01} = \frac{imE_0}{2\sqrt{2}\Omega\tau_M(1+K^2L_D^2)},$$

$$E^{+10} = \frac{m\Delta[E_D(1+K^2L_D^2)+E_0KL_0]/4}{1+K^2L_D^2+i\omega\tau_M[(1+K^2L_D^2)^2+K^2L_0^2]},$$

$$E^{+11} = \frac{-m\Delta(1+i\omega\tau_M)E_0/4\sqrt{2}\Omega\tau_M}{1+K^2L_D^2+i\omega\tau_M[(1+K^2L_D^2)^2+K^2L_0^2]}. \tag{15}$$

Here $E_0 = E_{ext}/\sqrt{2}$ is the effective value of the external electric field, $E_D = (k_BT/e)K$ is the diffusion field, $\sigma_0 = e\mu n_0$ is the average conductivity, $L_0 = \mu\tau E_0$ is the drift length of photocarriers, and $L_D = (k_BT\mu\tau/e)^{1/2}$ is the diffusion length.

Finally the expression for the complex amplitude of the photocurrent can be written as

$$j^\omega = \frac{-0.5m^2\Delta\sigma_0[E_D + E_0KL_0/(1+K^2L_D^2)]i\omega\tau_M}{1+i\omega\tau_M[1+K^2L_D^2+K^2L_0^2/(1+K^2L_D^2)]}. \tag{16}$$

Let us list the main features of the nonstationary holographic photocurrents excited in the ac external field. As follows from Eq. (16) the frequency transfer function of the effect has the traditional form typical for the diffusion mechanism of photocurrent excitation, namely, the linear growth of the signal for low modulation frequencies and the frequency-independent region for high frequencies of phase modulation.[8] These two regions are separated by a corresponding cutoff frequency,

$$\omega_0 = \frac{1}{\tau_M[1+K^2L_D^2+K^2L_0^2/(1+K^2L_D^2)]}. \tag{17}$$

For low spatial frequencies of the interference pattern (i.e., for $K^2L_D^2 \ll 1$) the most striking peculiarities can be observed. In this case the expressions for the photocurrent amplitude and corresponding cutoff frequency can be written as follows:

$$j^\omega = \frac{m^2\Delta}{2}\sigma_0 E_D \frac{-i\omega\tau_M(1+L_0^2/L_D^2)}{1+i\omega\tau_M(1+K^2L_0^2)}$$

$$= \frac{m^2\Delta}{2}\sigma_0 E_D \frac{-i\omega\tau_M(1+E_0^2/E_L^2)}{1+i\omega\tau_M(1+E_0^2/E_M^2)}, \tag{18}$$

$$\omega_0 = [\tau_M(1+K^2L_0^2)]^{-1} = [\tau_M(1+E_0^2/E_M^2)]^{-1}. \tag{19}$$

Here $E_L = k_BT/eL_D$, $E_M = (K\mu\tau)^{-1}$ are the characteristic values of the electric field.[3] As seen from Eq. (18) the dependence of the photocurrent amplitude on electric field has an S-like shape. The signal grows as E_0^2 between E_L and E_M due to the corresponding increase of the electric-field grating amplitudes E^{+00}, E^{+10} [Eq. (15)]. Beyond this region ($E_0 < E_L$, $E_0 > E_M$) the signal is independent on the electric field. The external field does not affect the photocurrent amplitude while the effective drift length is smaller than the diffusion one ($L_0 \ll L_D$). For high values of the applied electric field (the so-called long drift length regime) an enhanced transfer of electrons characterized by the large effective drift length L_0 takes place. Under these conditions the nonstationary photoconductivity grating is blurred leading to the saturation of the signal amplitude. The corresponding cutoff frequency ω_0 [Eq. (19)] falls down when drift length L_0 becomes comparable to the spatial period of the recorded grating ($L_0 \geqslant K^{-1}$ or $E_0 \geqslant E_M$).

The dependencies of the photocurrent amplitude j^ω and cutoff frequency ω_0 versus the ac field amplitude E_0 can be used for the determination of transport parameters of photoexcited carriers in semiconductor materials. Indeed, the characteristic breakpoints in these dependencies give the values of the diffusion and drift lengths of photocarriers and consequently the $\mu\tau$-product value.

We have also calculated the maximum gain of the photocurrent signal $j^\omega(\omega > \omega_0)$ which can be obtained in the sinusoidal ac field:

$$G_m = \frac{\lim\limits_{E_0\to\infty} j^\omega}{\lim\limits_{E_0\to 0} j^\omega} = \frac{1+K^2L_D^2+L_0^2/L_D^2}{1+K^2L_D^2+K^2L_0^2/(1+K^2L_D^2)}. \tag{20}$$

It depends on the spatial frequency of the interference pattern: $G_m = 1/K^2L_D^2$ for $K^2L_D^2 \ll 1$ and $G_m = 1$ for $K^2L_D^2 \gg 1$.

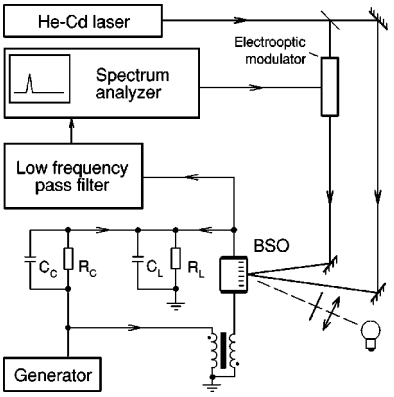

FIG. 2. Experimental setup for measurements of the nonstationary holographic photocurrents in the presence of alternating electric field.

III. EXPERIMENTAL SETUP

The experimental setup used for the measurements of the nonstationary holographic currents under applied alternating electric field is shown in Fig. 2. A standard He-Cd laser with an average power of $P_{out} \approx 1$ mW ($\lambda = 442$ nm) was used as the basic source of coherent radiation for formation of a recording interference pattern. To form the interference pattern with a specified fringe spacing and to cause its sinusoidal vibrations within the sample volume, we used a conventional Twyman-Green interferometer. An electro-optic phase modulator ML-102A produced phase modulation of the laser beam (with frequency ω and amplitude $\Delta = 0.16$). The voltage from the generator was amplified by conventional transformer and then applied to the crystal. The photocurrent signal was filtered and then measured by spectrum analyzer SK4-56 ($f = 0.01 - 50$ kHz, $\Delta f = 3$ Hz). In our experiments we used an *n*-type $Bi_{12}SiO_{20}$ crystal with characteristic dimensions $1 \times 3 \times 10$ mm^3; the front and back surfaces of the crystal (1×10 mm^2) were polished, and the silver paste electrodes (3×4 mm^2) were painted on the lateral surfaces. The interelectrode spacing was 1 mm. In order to change the parameters of the material (concentration of the trapping centers, characteristic recombination times, etc.[23]) the crystal was simultaneously illuminated by the light from the microscope lamp focused by lens and passed through the infrared filter KS-15 ($\lambda_{IR} = 650 - 2700$ nm, $I_{IR} = 13$ mW/mm^2).

IV. EXPERIMENTAL RESULTS

In this section we present the results of the photocurrent measurements carried out in the external electric field and compare them with the data obtained for the diffusion excitation regime. Figure 3 presents the frequency transfer function of the holographic photocurrent excited in the $Bi_{12}SiO_{20}$ crystal in the absence of an external electric field. Recall that the frequency response of the effect is usually characterized by the corresponding cutoff frequencies,[8]

$$\omega_0 = [\tau_M (1 + K^2 L_D^2)]^{-1}, \tag{21}$$

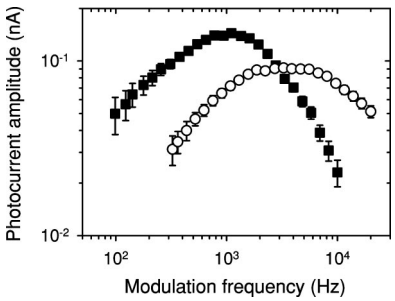

FIG. 3. Frequency transfer functions of the nonstationary photocurrent measured with (circles) and without (squares) additional infrared illumination ($Bi_{12}SiO_{20}$: $\lambda = 442$ nm, $E_0 = 0$, $P_0 = 0.32$ mW, $m = 0.65$, $K = 5 \times 10^4$ m^{-1}).

$$\omega_0' = (1 + K^2 L_D^2)\tau^{-1}. \tag{22}$$

From the dependencies of the photocurrent amplitude measured at low spatial frequency of the interference pattern ($K^2 L_D^2 \ll 1$) and without additional illumination we estimated corresponding cutoff frequencies: $\omega_0/2\pi \simeq 330$ Hz and $\omega_0'/2\pi \simeq 2.6$ kHz [Fig. 3 (squares)]. The present and earlier experiments[11] carried out in sillenite crystals (illumination wavelength $\lambda = 442$ nm) have revealed that the values of cutoff frequencies ω_0, ω_0' are close to each other. This means that the lifetime τ and Maxwell relaxation time τ_M are comparable: $\tau \sim \tau_M \sim 100$ μs.[11,12] In this case the cutoff frequencies are defined by more complicated expressions than those of Eqs. (21) and (22):[12]

$$\omega_0 = \frac{1 + \tau/\tau_I + K^2 l_D^2}{\tau + \tau_M (1 + \tau/\tau_I + K^2 L_D^2)}, \tag{23}$$

$$\omega_0' = \frac{1}{\tau_M} + \frac{1 + \tau/\tau_I + K^2 L_D^2}{\tau} + \frac{1 + \tau/\tau_I + K^2 l_D^2}{\tau + \tau_M (1 + \tau/\tau_I + K^2 L_D^2)}, \tag{24}$$

where τ_I is the lifetime of the ionized donor state, and l_D is the Debye screening length.

The condition $\tau \ll \tau_M$ is typical for most wide-gap semiconductor materials. To fulfill this condition and to conduct photocurrent measurements in the relaxation-time regime additional infrared illumination of the crystal ($\lambda_{IR} = 650 - 2700$ nm, $I_{IR} = 13$ mW/mm^2) was used. For the first and second cutoff frequencies the following values were obtained: $\omega_0/2\pi \simeq 800$ Hz ($\tau_M \simeq 0.25$ ms) and $\omega_0'/2\pi \simeq 13$ kHz ($\tau \simeq 12$ μs) [Fig. 3 (circles)]. As seen from Fig. 3 the second cutoff frequency ω_0' is remarkably shifted to higher excitation frequencies, which can be associated with the decrease of the electron lifetime. The growth of the first cutoff frequency ω_0 was clearly observed. This fact was unexpected since infrared illumination should not influence *stationary* photoconductivity of the crystal (and correspondingly the value of the Maxwell relaxation time). Note that even a 20% – 25% *decay* of the sample's conductance in the presence of the infrared light was observed. For this reason the behavior of ω_0 cannot be attributed to the growth of the conductivity. The observed behavior can be explained by the

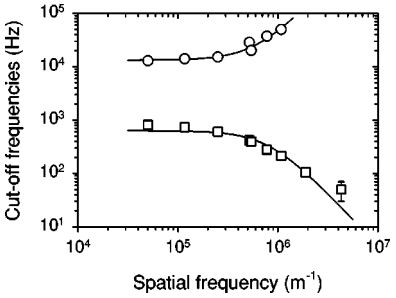

FIG. 4. Dependence of the cutoff frequencies ω_0 (squares), ω_0' (circles) on the spatial frequency K of the interference pattern ($Bi_{12}SiO_{20}$: $\lambda=442$ nm, $E_0=0$, $P_0=0.32$ mW, $m=0.65$; infrared illumination is switched on). The theoretical curves are calculated using Eqs. (21) and (22).

fact that $\tau\sim\tau_M$. In this case the cutoff frequency depends both on the electron lifetime and the Maxwell relaxation time. The former vanishes with the additional illumination resulting in the slight change of the first cutoff frequency.

The dependencies of the corresponding cutoff frequencies versus spatial frequency of the interference pattern K are presented in Fig. 4. The experimental dependencies were fitted using Eqs. (21) and (22) providing the following estimations for the diffusion length of photocarriers: $L_D\simeq 1.2$ μm ($\mu\tau\simeq 0.6\times 10^{-10}$ m^2/V) [from $\omega_1(K)$], $L_D\simeq 1.6$ μm ($\mu\tau\simeq 1.0\times 10^{-10}$ m^2/V) [from $\omega_2(K)$].

Investigation of the spatial frequency dependence of the holographic photocurrent gives another possibility for the diffusion length determination. For the diffusion mechanism of recording ($E_0=0$) and for modulation frequencies higher than the first characteristic cutoff frequency ($\omega>\omega_0$) the simplest theory of the effect predicts the following dependence of the photocurrent amplitude versus spatial frequency:[8]

$$j^{\omega}(K)\propto\frac{K}{1+K^2L_D^2}. \tag{25}$$

We performed these measurements (Fig. 5) and obtained the following estimation for the diffusion length of electrons: $L_D=1.4$ μm ($\mu\tau\simeq 0.7\times 10^{-10}$ m^2/V).

Let us proceed to the case of nonzero alternating electric field applied to the crystal. The frequency dependence of the

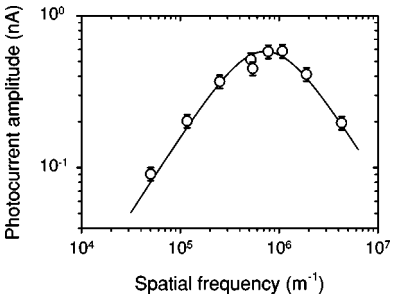

FIG. 5. Dependence of the photocurrent amplitude $|J^{\omega}|$ on the spatial frequency K ($Bi_{12}SiO_{20}$, $\lambda=442$ nm, $E_0=0$, $P_0=0.32$ mW, $m=0.65$; infrared illumination is switched on). The solid line shows the theoretical curve calculated using Eq. (25).

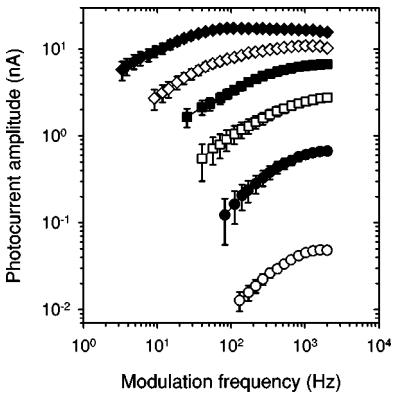

FIG. 6. Frequency transfer functions of the photocurrent measured for $E_0=0$ (open circles), 53 V/mm (filled circles), 130 V/mm (open squares), 210 V/mm (filled squares), 410 V/mm (open diamonds), and 1000 V/mm (filled diamonds). $Bi_{12}SiO_{20}$: $\lambda=442$ nm, $P_0=0.19$ mW, $m=0.65$, $K=5\times 10^4$ m^{-1}, and infrared illumination is switched on.

photocurrent amplitude measured for different values of electric field applied to the crystal is presented in Fig. 6. As seen from this figure all dependencies keep the form typical for the diffusion mechanism of the photocurrent excitation. No resonant peaks on the frequency response were observed even for the highest voltage applied. The giant enhancement of the signal amplitude is another feature of the nonstationary photocurrent excitation in an external ac electric field (Figs. 6 and 7). The characteristic growth of the signal amplitude as $\propto E_0^2$ was observed in the region $E_0=(0.2-2)\times 10^5$ V/m. The photocurrent amplification by a factor of $G_m\simeq 350$ (~ 50 dB) has been achieved for low spatial frequencies of the interference pattern ($K^2L_D^2\ll 1$). This value is even higher than the theoretical estimation of the maximum gain factor by Eq. (20): $G_m=140-280$ ($K=5\times 10^4$ m^{-1}, $L_D=1.2-1.7$ μm).

The $\mu\tau$ product or diffusion length of photocarriers can be estimated from both the characteristic breakpoints on the dependence of the photocurrent amplitude versus ac field amplitude (Fig. 7). We have approximated this dependence by Eq. (18) and obtained the following values: $E_L\simeq 1.5$

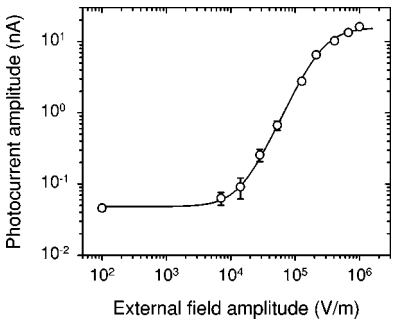

FIG. 7. Photocurrent amplitude $|J^{\omega}|$ ($\omega>\omega_0$) versus effective value of the external ac field E_0 ($Bi_{12}SiO_{20}$: $\lambda=442$ nm, $P_0=0.19$ mW, $m=0.65$, $K=5\times 10^4$ m^{-1}, $\omega/2\pi=2.0$ kHz; infrared illumination is switched on). The measurement performed at zero field is shown at $E_0=10^2$ V/m. The solid line shows the theoretical curve calculated using Eq. (18).

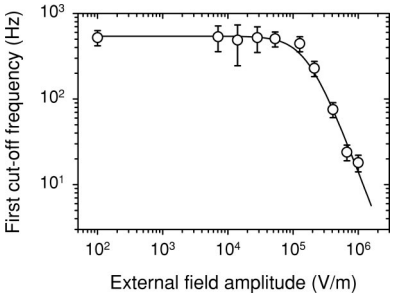

FIG. 8. Dependence of the cutoff frequency ω_0 on the effective value of the external ac field E_0 ($Bi_{12}SiO_{20}$: $\lambda = 442$ nm, $P_0 = 0.19$ mW, $m = 0.65$, $K = 5\times10^4$ m^{-1}; infrared illumination is switched on). The measurement performed at zero field is shown at $E_0 = 10^2$ V/m. The approximation using Eq. (19) is shown by the solid line.

$\times10^4$ V/m ($L_D \simeq 1.7$ μm, $\mu\tau \simeq 1.2\times10^{-10}$ m^2/V) for the first breakpoint and $E_M \simeq 2.6\times10^5$ V/m ($L_D \simeq 1.4$ μm, $\mu\tau \simeq 0.8\times10^{-10}$ m^2/V) for the second breakpoint.

The behavior of the the first cutoff frequency ω_0 versus applied electric field is similar to the drift mechanism of recording—it shifts towards low excitation frequencies (Fig. 8). Approximation of this dependence by Eq. (19) provides the value of $\mu\tau$ product: $\mu\tau \simeq 1.2\times10^{-10}$ m^2/V ($E_M \simeq 1.6\times10^5$ V/m).

V. DISCUSSION

The utilization of ac field for the photocurrent signal enhancement provides several important advantages over the application of dc field. First, the flat frequency response of the effect seems to be more convenient for measurements of phase-modulated optical signals of small amplitude. The high-frequency alternating electric field ($\Omega \gg \tau_M^{-1}$) applied to the crystal is more homogeneous than the dc field (no screening effects are presented).[23] For this reason the measurements performed in fast ac fields are expected to be more plausible.

Determination of the $\mu\tau$ product from the dependence of photocurrent amplitude versus applied ac voltage is much easier than the standard technique based on the measurements of the photocurrent amplitude on the spatial frequency of the interference pattern, which is a time consuming operation and includes numerous mechanical movements and readjustments of optical components (see, for example, Ref. 8). The position of the first breakpoint on the dependence $J^{\omega}(E_0)$, i.e., E_L (see Sec. II), does not depend both on spatial frequency of the interference pattern K (for $K^2L_D^2 \ll 1$) and average light intensity I_0, which minimizes corresponding experimental errors.

To summarize, we have analyzed the influence of the alternating electric field on the nonstationary photocurrent amplitude and dynamics of space-charge gratings in semiconductor materials. The simple technique for the $\mu\tau$-product determination is proposed. The nonresonant enhancement of the signal of $\sim$50 dB has been achieved in *n*-type $Bi_{12}SiO_{20}$. We believe that influence of an ac external electric field is not restricted to the considered cases. The proposed technique can be used for characterization of other photoconductive crystals (e.g., semi-insulating ZnSe, GaN) with different material constants, where the characteristic breakpoints will be observed at other values of the applied field.

*Electronic address: i.a.sokolov@pop.ioffe.rssi.ru

[1] M.P. Petrov, S.I. Stepanov, and A.V. Khomenko, *Photorefractive Crystals in Coherent Optical Systems* (Springer-Verlag, Berlin, 1991).
[2] S.I. Stepanov, V.V. Kulikov, and M.P. Petrov, Opt. Commun. **44**, 19 (1982).
[3] Ph. Refregier, L. Solymar, H. Rajbenbach, and J.P. Huignard, J. Appl. Phys. **58**, 45 (1985).
[4] S.I. Stepanov and M.P. Petrov, Opt. Commun. **53**, 292 (1985).
[5] J. Kumar, G. Albanese, and W.H. Steier, J. Opt. Soc. Am. B **4**, 1079 (1987).
[6] K. Walsh, A.K. Powell, C. Stace, and T.J. Hall, J. Opt. Soc. Am. B **7**, 288 (1990).
[7] G.S. Trofimov and S.I. Stepanov, Fiz. Tverd. Tela (Leningrad) **28**, 2785 (1986) [Sov. Phys. Solid State **28**, 1559 (1986)].
[8] M.P. Petrov, I.A. Sokolov, S.I. Stepanov, and G.S. Trofimov, J. Appl. Phys. **68**, 2216 (1990).
[9] G.S. Trofimov, A.I. Kosarev, A.G. Kovrov, and P.G. LeComber, J. Non-Cryst. Solids **137-138**, 483 (1991).
[10] U. Haken, M. Hundhausen, and L. Ley, Phys. Rev. B **51**, 10 579 (1995).
[11] I.A. Sokolov and S.I. Stepanov, Electron. Lett. **26**, 1275 (1990).
[12] I.A. Sokolov and S.I. Stepanov, Optik (Stuttgart) **93**, 175 (1993).
[13] I.A. Sokolov and S.I. Stepanov, J. Opt. Soc. Am. B **10**, 1483 (1993).
[14] S. Mansurova, S. Stepanov, N. Korneev, and C. Dibon, Opt. Commun. **152**, 207 (1998).
[15] M.A. Bryushinin and I.A. Sokolov, Phys. Rev. B **63**, 153203 (2001).
[16] S.I. Stepanov, I.A. Sokolov, G.S. Trofimov, V.I. Vlad, D. Popa, and I. Apostol, Opt. Lett. **15**, 1239 (1990).
[17] D.M. Pepper, Opt. Photonics News **8**, 33 (1997).
[18] P. Rodriguez and S. Stepanov, in *Summaries of the Conference on Lasers and Electro-Optics (CLEO'97), May 18–23, 1997, Baltimore, 1997*, OSA Technical Digest Series, Vol. 11, Conference edition (Optical Society of America, Washington, 1997), p. 45.
[19] P.M. Johansen and H.C. Pedersen, J. Opt. Soc. Am. B **15**, 1366 (1998).
[20] I.A. Sokolov and S.I. Stepanov, Appl. Opt. **32**, 1958 (1993).
[21] L. Solymar, D.J. Webb, and A. Grunnet-Jepsen, *The Physics and Applications of Photorefractive Materials* (Oxford University Press, New York, 1996).
[22] J. Takacs and L. Solymar, Opt. Lett. **17**, 247 (1992).
[23] S.M. Ryvkin, *Photoelectric Effects in Semiconductors* (Consultants Bureau, New York, 1964).